

Supplementary Material

Supplementary Figures and Tables

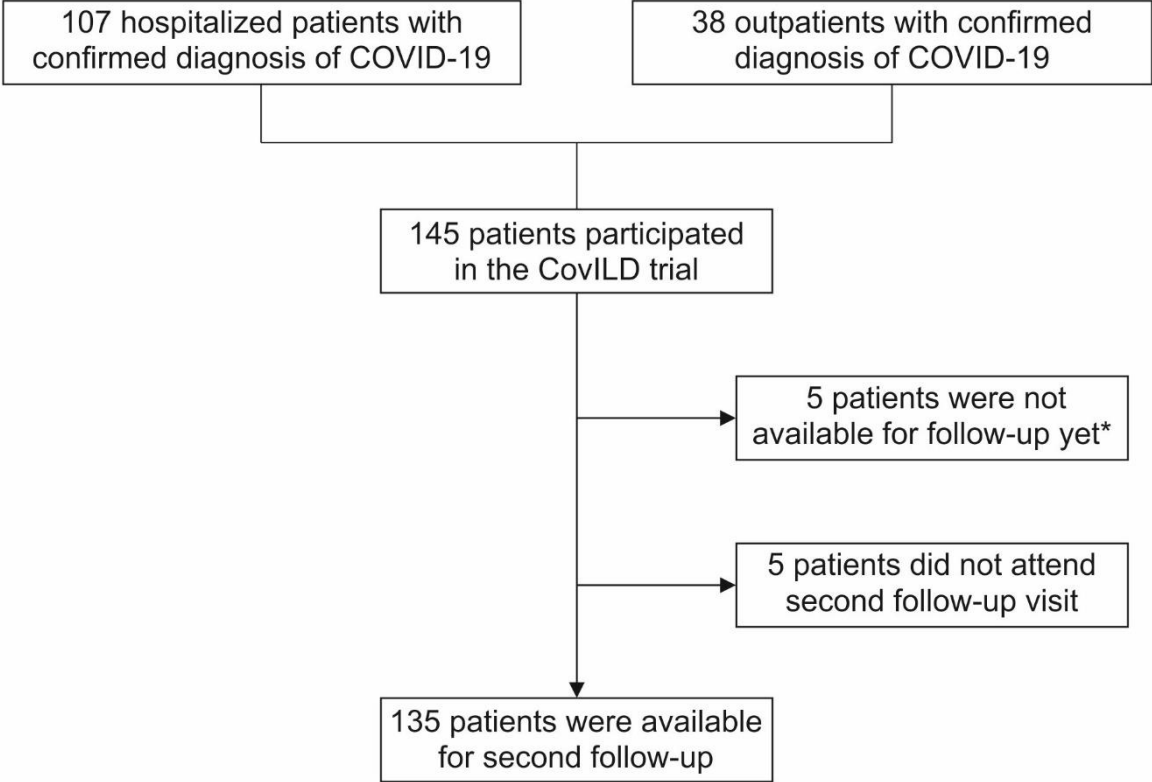


Figure S1: Enrollment of CovILD study participants

*non-available patients have not attended the second follow-up (V2=100 days post COVID-19 diagnosis) yet.

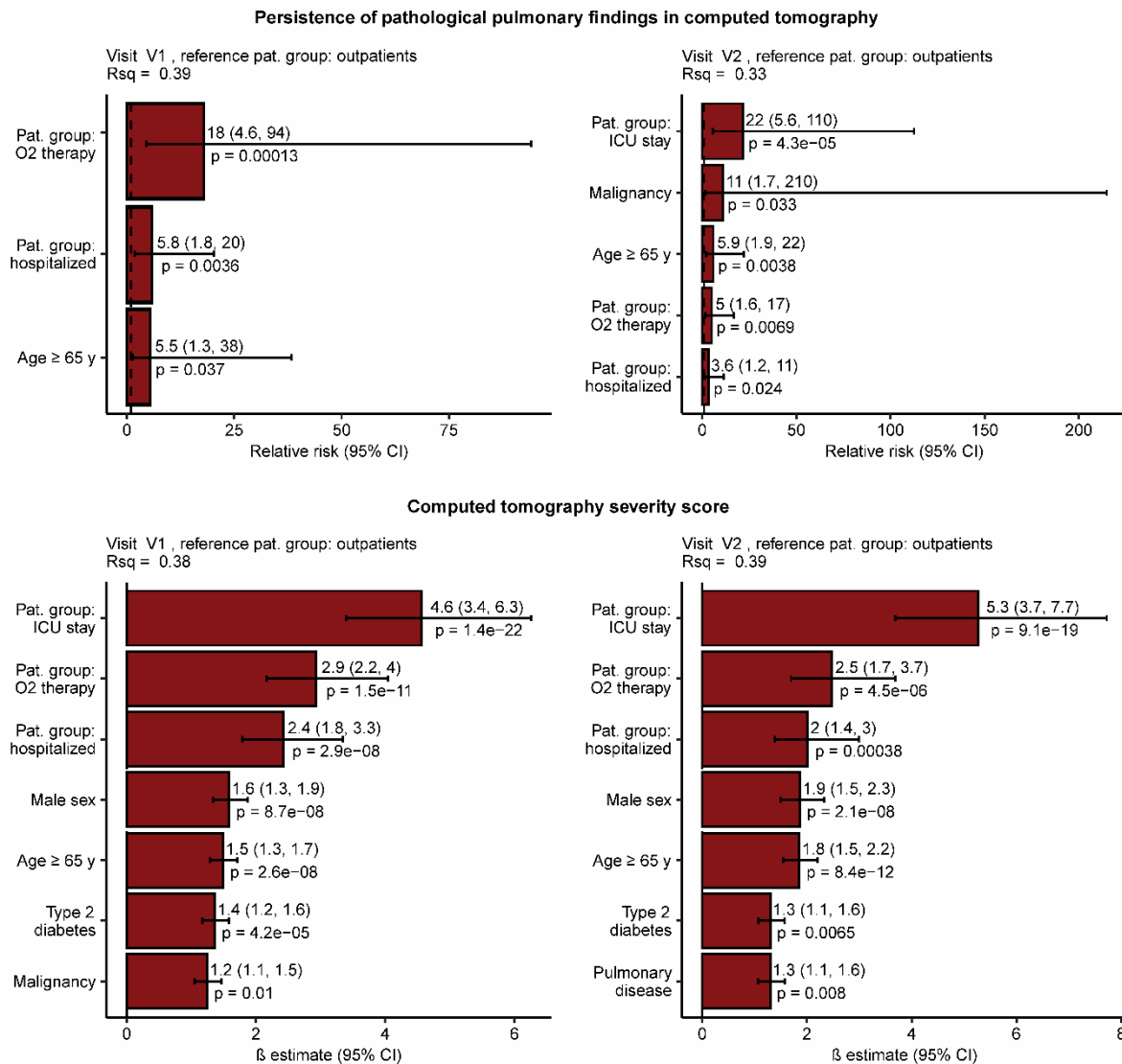


Figure S2 Demographic and clinical factors impacting the persistence of radiological lung findings

To identify demographic and clinical factors impacting on the persistence of radiological lung findings at visit 1 and visit 2 a series of fixed-effect generalized linear models (presence of pathological CT findings (yes/no): logistic regression; CT severity score (points): generalized linear model with log link function and assumed Poisson distribution of residuals) were created to analyze the persistence and severity of lung pathologies in computed tomography at follow-up. The dependent variables of the models were patient treatment group (outpatient, hospitalized without respiratory support, hospitalized with oxygen supply, mechanical ventilation), sex, age ≥ 65 years, obesity, smoking history, presence of cardiovascular diseases, hypertension, pulmonary diseases, hypercholesterolemia, type 2

diabetes, and malignancy. Significant coefficients of the optimized models ($\exp \beta$) were presented as bar plots with whiskers representing the 95% confidence interval and p values ($\beta \neq 0$; Wald Z test). Visit 1 = 60 days and visit 2 = 100 days after diagnosis of COVID-19; N=145.

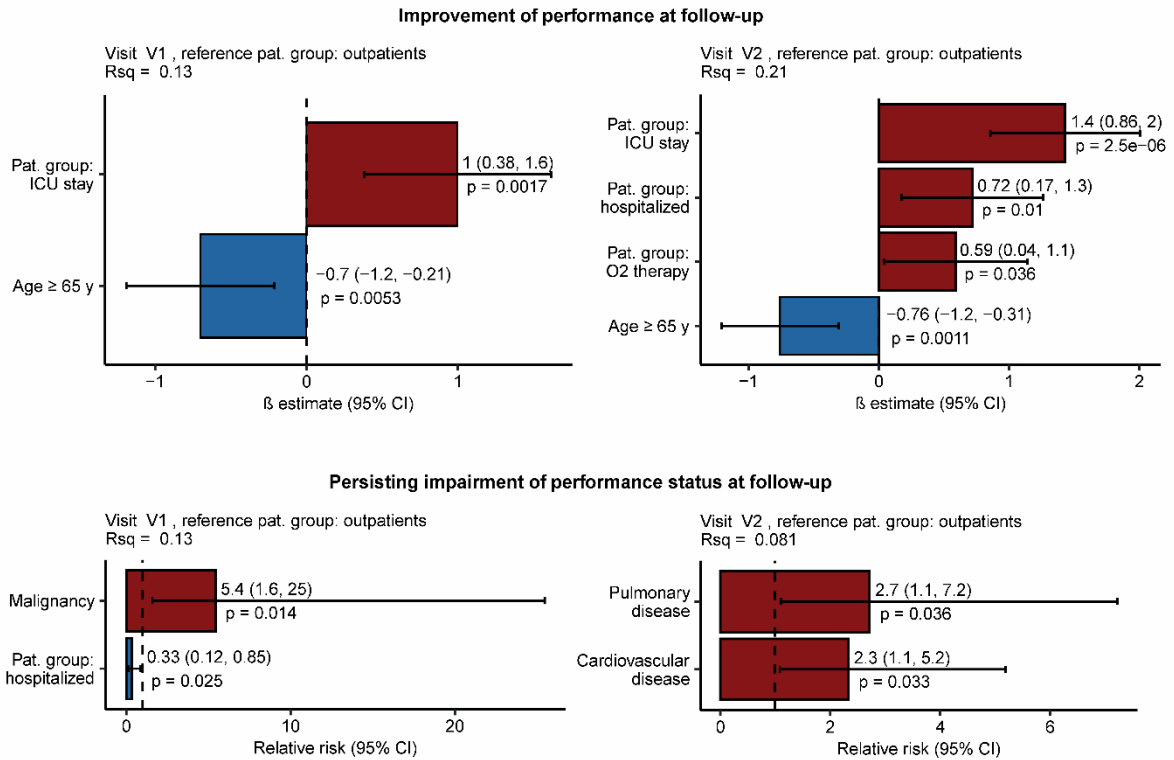


Figure S3 Demographic and clinical factors impacting patient performance status at follow-up

To identify demographic and clinical factors impacting patient performance status (assessed via self-report) at visit 1 and visit 2 a series of fixed-effect ordinary and generalized linear models were created for the key investigated parameters (change of performance status: ordinary linear model; impaired performance: logistic regression). The dependent variables of the models were patient treatment group, sex, age \geq 65 years, obesity, smoking history, presence of cardiovascular diseases, hypertension, pulmonary diseases, hypercholesterolemia, type 2 diabetes, and malignancy. Significant coefficients of the optimized models (β for ordinary linear models, $\exp \beta$ for logistic regression) were presented as bar plots with whiskers representing the 95% confidence interval and p values ($\beta \neq 0$; two-tailed T-test for ordinary linear models, Wald Z test for generalized linear models). Visit 1 = 60 days and visit 2 = 100 days after diagnosis of COVID-19; N=145.

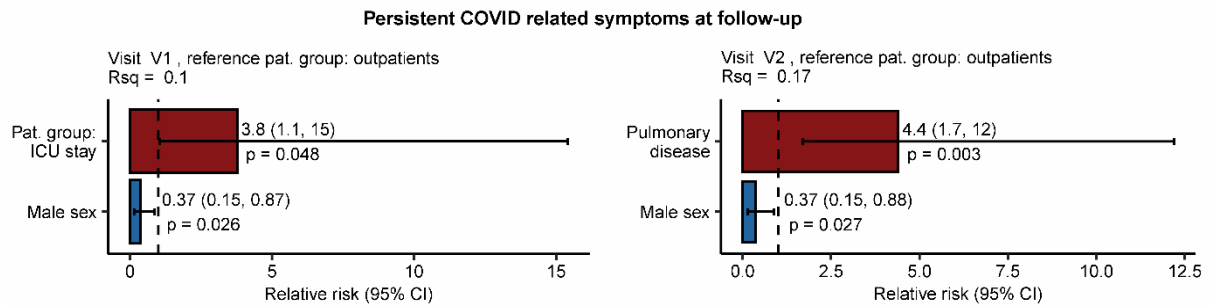


Figure S4 Demographic and clinical factors impacting the persistence of COVID-19 related symptoms

To identify demographic and clinical factors impacting the persistence of symptoms at visit 1 and visit 2 logistic regression analysis was performed. The dependent variables of the models were patient treatment group, sex, age ≥ 65 years, obesity, smoking history, presence of cardiovascular diseases, hypertension, pulmonary diseases, hypercholesterolemia, type 2 diabetes, and malignancy. Significant coefficients of the optimized models ($\exp \beta$) were presented as bar plots with whiskers representing the 95% confidence interval and p values ($\beta \neq 0$; Wald Z test). Visit 1 = 60 days and visit 2 = 100 days after diagnosis of COVID-19; N=145.

Table S1: Demographics and clinical characteristics of patients enrolled in CovILD according to acute disease severity

	Mild N=36	Moderate N=37	Severe N=40	Critical N=32	p-value
Characteristics					
Mean age – yr (SD)	46 (14)	60 (13)	64 (13)	59 (9)	<0.001
Female sex – no. (%)	26 (72)	22 (60)	6 (15)	9 (28)	<0.001
Mean body mass index – kg/m ² (SD)*	25 (5)	26 (4)	28 (6)	27 (4)	0.109
Smoking history – no. (%)	8 (22)	16 (43)	23 (58)	10 (31)	0.011
Current – no. (%)	1 (3)	3 (8)	0 (0)	0 (0)	0.112
Mean pack years – no. (SD)	2 (5)	11 (21)	13 (17)	6 (13)	0.002
Comorbidities – no. (%)					
None	19 (53)	6 (16)	5 (13)	3 (9)	<0.001
Cardiovascular disease	3 (8)	11 (30)	25 (63)	19 (59)	<0.001
Hypertension	3 (8)	7 (19)	18 (45)	16 (50)	<0.001
Pulmonary disease	6 (17)	9 (24)	7 (18)	5 (16)	0.775
COPD	2 (6)	2 (5)	2 (5)	2 (6)	0.997
Asthma	3 (8)	3 (8)	1 (3)	3 (9)	0.635
Interstitial lung disease#	0 (0)	1 (3)	0 (0)	0 (0)	0.401
Metabolic disease	8 (22)	16 (43)	22 (55)	17 (53)	0.019
Hypercholesterolemia	2 (6)	7 (19)	13 (33)	5 (16)	0.025
Diabetes mellitus, type 2	1 (3)	6 (16)	8 (20)	9 (28)	0.039
Chronic kidney disease	0 (0)	0 (0)	4 (10)	6 (19)	0.005
Chronic liver disease	1 (3)	1 (3)	3 (8)	3 (9)	0.513
Malignancy	2 (6)	5 (14)	7 (18)	3 (9)	0.408
Immunodeficiency	1 (3)	2 (5)	0 (0)	6 (19)	0.007

*The body-mass index is the weight kilograms divided by the square of the height in meters. # one patient with a history of radiation-induced pneumonitis, Disease severity is depicted according to the need for medical treatment during acute COVID-19: mild = outpatient, moderate = hospitalization without respiratory support, severe = hospitalization with the need for oxygen supply, critical = ICU treatment with mechanical ventilation. Comparisons according to acute disease severity were calculated with Kruskal-Wallis or Chi-Square test.

Table S2: Echocardiography of COVID-19 patients at follow-up

	First follow-up	Second follow-up	p-value time change
LVEF reduced – no. (%) [*]	4 (3)	4 (3)	1.000
Signs of pulmonary hypertension – no. (%) [#]	14 (10)	13 (10)	1.000
Diastolic dysfunction – no. (%) [‡]	87 (60)	73 (55)	0.405
Pericardial effusion – no. (%)	8 (6)	1 (1)	0.039

^{*}LVEF, left ventricular ejection fraction as determined by Simpson method, a LVEF below 53% was considered to be reduced.

[#]indirect signs of pulmonary hypertension were assessed by measurement of tricuspid annular plane systolic excursion (TAPSE), right atrial area (RAA), systolic pulmonary arterial pressure (sPAP), maximal tricuspid regurgitation velocity (TRVmax), left ventricular end-systolic eccentricity index (Lei-Index, defined as the ratio of the anterior-inferior and septal-posterolateral cavity dimensions at the mid-ventricular level) and right-ventricular diameters. If all parameters were normal no pulmonary hypertension was suspected.

[‡]assessed via E/A and E'/A' ratios. Neman test was applied to calculate time-dependent changes. The first follow-up took place 60 days after COVID-19 diagnosis, the second follow-up was performed 100 days after COVID-19 diagnosis. Echocardiography data were available for 145 patients at first follow-up and 134 patients at the second follow-up.

Table S3 Laboratory parameters of COVID-19 patients at follow-up

	First follow-up	Second follow-up	p-value time change
C-reactive protein – mg·dL ⁻¹	0.4 ± 1.0	0.3 ± 0.6	0.192
Interleukin 6 – mg·dL ⁻¹	3.8 ± 6.4	3.0 ± 2.5	0.443
Pro-calcitonin – µg*L ⁻¹	0.07 ± 0.02	0.07 ± 0.02	0.478
D-dimer – µg*L ⁻¹	750 ± 1398	564 ± 804	<0.001
NT-proBNP – mg*dL ⁻¹	240 ± 523	181 ± 313	0.006
Ferritin – µg*L ⁻¹	259 ± 236	192 ± 184	<0.001
Transferrin saturation – %	25 ± 10	24 ± 9	0.067
Hemoglobin – g*L ⁻¹	138 ± 15	141 ± 16	<0.001

Data are depicted as mean ± SD. Wilcoxon signed-rank tests were applied to assess time-dependent changes. The first follow-up took place 60 days after COVID-19 diagnosis; the second follow-up was performed 100 days after COVID-19 diagnosis. Blood samples were available from 145 patients at the first follow-up and 134 patients at the second follow-up.

Table S4: Distribution of pathological pulmonary findings assessed with computed tomography

	First follow-up	Second follow-up
Bilateral – no. (%)	84 (67)	68 (50)
Right upper lobe – no. (%)	67 (53)	39 (42)
Right middle lobe – no. (%)	57 (45)	45 (33)
Right lower lobe – no. (%)	84 (67)	75 (56)
Left upper lobe – no. (%)	65 (52)	31 (33)
Left lower lobe – no. (%)	84 (67)	48 (52)

The first follow-up took place 60 days after COVID-19 diagnosis; the second follow-up was performed 100 days after COVID-19 diagnosis. CT scans of the lung were available from 145 patients at the first follow-up and 135 patients at the second follow-up.

Supplementary Methods

Statistics

Data transformation and statistical analysis were done with R programming suite version 3.6.3 with the *tidyverse* package bundle [1]. Statistical significance of differences of the investigated parameters between the study visits was assessed by mixed-effect linear modeling (fixed effect: study visit, random effect: study participant, R package *lmer*) and p values of the study visit effect estimates were presented ($\beta \neq 0$; two-tailed T-test for ordinary mixed-effect models, Wald Z test for generalized mixed-effect linear models) [2]. For normally distributed continuous parameters, canonical mixed-effect linear regression was applied. For CT severity score, mixed-effect generalized linear models with log link function and assumed Poisson distribution of residuals were used. Binary parameters were modeled with mixed-effect logistic regression (logit link function, assumed binomial distribution of residuals). In modeling tasks investigating the baseline difference in parameters between patients with various history of acute COVID-19 severity (according to the need for medical treatment), the patient severity group term was included, where the patient severity groups were defined as follows: (1) outpatients (n = 36), (2) hospitalized subjects without oxygen therapy or ICU stay (n = 37), (3) hospitalized participants with oxygen therapy but without ICU stay (n = 40) and (4) ICU patients (n = 32).

To identify demographic and clinical factors impacting the persistence of symptoms and radiological lung findings at visit 1 and visit 2 a series of fixed-effect ordinary and generalized linear models were created for the key investigated parameters (change of performance status: ordinary linear model; impaired performance, presence of persistent symptoms and presence of CT abnormalities: logistic regression; CT severity score: generalized linear model with log link function and assumed Poisson distribution of residuals). The dependent binary variables of the models were patient treatment group, sex, age ≥ 65 years, obesity, smoking history, presence of cardiovascular diseases, hypertension, pulmonary diseases, hypercholesterolemia, type 2 diabetes, and malignancy. The raw full models were optimized

by an initial automated removal of non-relevant terms using the *stepAIC* function of *MASS* package, followed by manual step-wise elimination of non-significant terms based on the results of the likelihood ratio test (LRT) [3, 4]. The R-squared value of the optimized models was calculated with the *rsq* function from the *rsq* package [5]. Significant coefficients of the optimized models (β for ordinary linear models, $\exp \beta$ for generalized linear models/logistic regression) were presented as bar plots with whiskers representing the 95% confidence interval and p values ($\beta \neq 0$; two-tailed T-test for ordinary linear models, Wald Z test for generalized linear models) using the *ggplot2* package [6].

Supplementary References

1. Wickham H, Averick M, Bryan J, Chang W, McGowan L, François R, Golemund G, Hayes A, Henry L, Hester J, Kuhn M, Pedersen TL, Miller E, Bache SM, Müller K, Ooms J, Robinson D, Seidel DP, Spinu V, Takahashi K, Vaughan D, Wilke C, Woo K, Yutani H. Welcome to the Tidyverse. *The Journal of Open Source Software* 2019; 4 (43): 1686.
2. Bates D, Mächler BM, Bolker SC. *Journal of Statistical Software* 2015; 67: 1-48.
3. Venables WN, Ripley BD. *Modern Applied Statistics with S*. Springer, 2002.
4. Crawley MJ. *Statistics: An Introduction using R*. John Wiley & Sons, Ltd, 2011.
5. Zhang DB. A Coefficient of Determination for Generalized Linear Models. *Am Stat* 2017; 71(4): 310-316.
6. Wickham H. *ggplot2: Elegant Graphics for Data Analysis*. 1st ed. Springer Verlag, 2016.